



# Distinct Element Modelling of Constant Stress Ratio Compression Tests on Pore-Filling Type Methane Hydrate Bearing Sediments

Mingjing Jiang<sup>1,2,3(✉)</sup>, Wenkai Zhu<sup>1,2,3</sup>, and Jie He<sup>4</sup>

<sup>1</sup> Department of Geotechnical Engineering, College of Civil Engineering, Tongji University, Shanghai 200092, China

mingjing.jiang@tongji.edu.cn

<sup>2</sup> Key Laboratory of Geotechnical and Underground Engineering of Ministry of Education, Tongji University, Shanghai 200092, China

<sup>3</sup> State Key Laboratory of Disaster Reduction in Civil Engineering, Tongji University, Shanghai 200092, China

<sup>4</sup> Shanghai Jianke Engineering Consulting Co., Ltd., Shanghai 200092, China

**Abstract.** The mechanical behavior of methane hydrate bearing sediments (MHBS) subjected to various stress-path loading is relevant to seabed subsidence or hydrate sediment strata deformation and well stability during the exploration and methane exploitation from methane hydrate (MH) reservoir. This study presents a numerical investigation into the mechanical behavior of pore-filling type MHBS along constant stress ratio path using the distinct element method (DEM). In the simulation, methane hydrate was modelled as agglomerates of sphere cemented together in the pores of soils. The numerical results indicate that the compressibility of MHBS is low before yielding but higher after. Bond breakage in MH agglomerates occurs during loading and the bond contact ratio decreases when the major principal stress increases. As for the fabric tensors, the minor principal fabric slightly increases to a constant value while the major principal fabric decreases to a constant value.

**Keywords:** Methane hydrate bearing sediments · Distinct element method  
Pore-filling · Constant stress ratio compression test · Bond breakage

## 1 Introduction

Methane hydrate (MH) is a crystalline solid in which methane molecules are captured by cages formed by water molecules framework under high pressure and low temperature [1]. Methane hydrate bearing sediments (MHBS) is a soil deposit containing MH in its pores. The exploration of MH has attracted worldwide attention for its high energy density. However, MHs only exist stably under certain conditions and changes of pore pressure or temperature caused by gas exploitation may lead to MH dissociation, which may change the mechanical properties of MHBS and trigger a series of and geo-hazards. Therefore, a deep investigation on the mechanical behaviors of MHBS is necessary.

The mechanical behavior of MHBS is influenced by many factors, among which the formation of MHs in the pore of MHBS plays an important role. According to previous research, three formation habits of MHs have been summarized: pore-filling, cementation and load-bearing [2]. In the last decades, considerable laboratory tests have been conducted to study the mechanical properties of natural and artificial MHBS, such as triaxial compression tests [3, 4] and direct shear tests [5]. However, the mechanical behavior of MHBS is still insufficient, especially the microscopic mechanism related with the macroscopic behavior. The distinct element method (DEM) [6] is efficient to capture the evolution of microscopic particle interactions and thus was employed. In this study, a pore-filling types of MHBS was generated by a novel technique. The constant stress ratio (CSR) compression tests with different stress ratios are performed to analyze its volumetric strain and contact fabric.

## 2 Numerical Simulation

A new technique proposed by He and Jiang [7] was used to generate the pore-filling type MHBS samples. At first, a cubic sample with an initial void ratio of 0.84 was generated by multi-layer under-compaction method (UCM) [8]. The size of the sample is  $5.445 \times 5.445 \times 5.445 \text{ mm}^3$ . The grain size distribution is similar to that of Toyoura sand.

After the generation,  $N$  particles with radius of  $R_a$  was randomly created in the pores of soil particles according to the MH saturation  $S_{mh}$  which is defined by the ratio of MH volume  $V_{mh}$  to the total pore volume  $V_v$ . Subsequently, the particle with radius of  $R_a$  was replaced by a near-spheroidal cluster, which was formed by bonding  $n$  MH particles with radius  $r$  together. The void ratio of the cluster is  $e_a$ . The number of MH clusters  $N$  can be calculated by:

$$N = \frac{V_{mh}}{\frac{4}{3}n\pi r^3 \times (1 + e_a)} \quad (1)$$

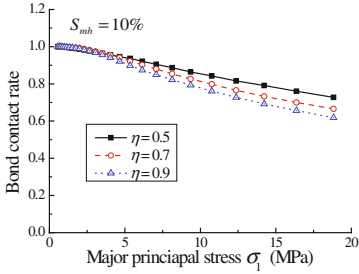
In this study, the void ratio of the MH cluster  $e_a$  is 0.82, the radius of the MH particle  $r$  is 0.024 mm and the number of MH particles in a cluster  $n$  is set to 60. When  $S_{mh} = 10\%$ , the number of MH clusters  $N$  is 1166. The parallel bond model (BPM) is employed in the cluster and the material parameters used in this paper is the same as in [9].

## 3 Numerical Results

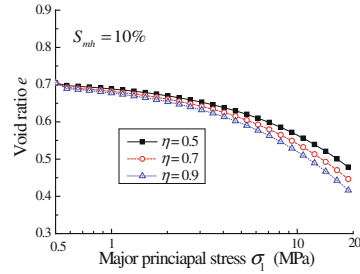
In CSR tests, the intermediate principal stress  $\sigma_2$  and the minor principal stress  $\sigma_3$  were kept equal and the stress ratio  $\eta$  was maintained constant, i.e.,  $\sigma_2 = \sigma_3 = \eta\sigma_1$ . The load was applied step by step. In the first step,  $\sigma_1$  was set to 1.0 MPa and the latter  $\sigma_1$  was 1.15 times the former  $\sigma_1$  during the subsequent loading. To investigate the influence of stress ratio, three different stress ratio, i.e., 0.5, 0.7, 0.9, were used.

Figure 1 shows relationships between void ratio and major principal stress of MHBS with  $S_{mh} = 10\%$  under different stress ratios. The void ratio decreases when the major

principal stress increases. And the compressibility of pore-filling type MHBS is low before yielding but higher after, though the yield point is not obvious. Besides, the void ratio is lower when stress ratio is higher, which indicates that the yield of the MHBS sample is related to stress path.



**Fig. 1.** Relationships between void ratio and major principal stress of MHBS with  $S_{mh} = 10\%$  under different stress ratios.



**Fig. 2.** Relationships between bond contact rate and major principal stress of MHBS with  $S_{mh} = 10\%$  under different stress ratios.

Relationships between bond contact ratio and major principal stress of MHBS with  $S_{mh} = 10\%$  under different  $\eta$  is illustrate in Fig. 2. The bond contact ratio is defined as the ratio of bond contact number to initial bond contact number. The bond contact ratio decreases when the major principal stress increases.

The fabric tensor is defined based on Satake [10] to describe the soil anisotropy:

$$F_{ij} = \frac{1}{N_c} \sum_{k=1}^{N_c} n_i^k n_j^k, i = j = 1, 3 \tag{2}$$

where  $N_c$  is the contact number,  $n_i^k$  is the component of the unit vector  $n^k$  at a contact.

The fabric tensor for the strong contacts is described by [11]:

$$F_{ij}^s = \frac{1}{N_c^s} \sum_{s=1}^{N_c^s} n_i^s n_j^s, i = j = 1, 3 \tag{3}$$

where  $N_c^s$  is the number of the strong contacts and  $n_i^s$  is the component of unit vector  $n^s$  at a strong contact.

The development of the eigenvalues of contacts ( $F_{11}, F_{22}, F_{33}$ ) for MHBS samples with  $S_{mh} = 10\%$  when  $\eta = 0.7$  during the test is presented in Fig. 3(a). It can be seen that the minor principal fabric  $F_{33}$  slightly increases to a constant value while the major principal fabric  $F_{11}$  slightly decreases to a constant value. As for the eigenvalues of the strong contacts ( $F_{11}^s, F_{22}^s, F_{33}^s$ ), shown in Fig. 3(b),  $F_{11}^s$  reaches a peak value then decreases, while  $F_{22}^s$  and  $F_{33}^s$  decrease to a minimum value then increase.

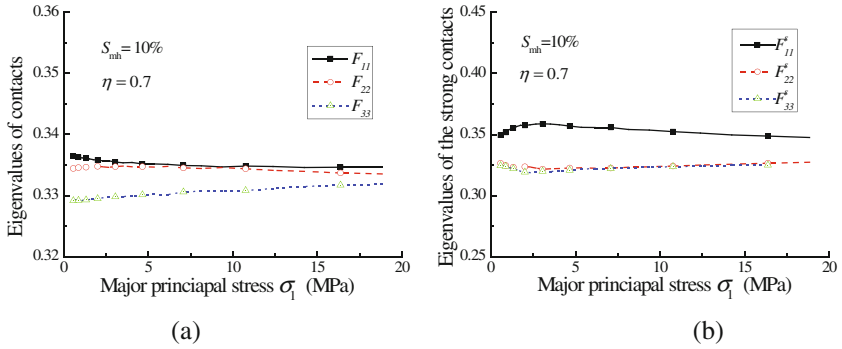


**Fig. 3.** The development of the eigenvalues of (a) contacts and (b) the strong contacts for MHBS samples with  $S_{mh} = 10\%$  when  $\eta = 0.7$ .

## References

1. Max, M.D., Lowrie, A.: Oceanic methane hydrates: a “frontier” gas resource. *J. Pet. Geol.* **19**(1), 41–56 (1996)
2. Waite, W.F., Santamarina, J.C., Cortes, D.D., et al.: Physical properties of hydrate-bearing sediments. *Rev. Geophys.* **47**, 38 (2009)
3. Hyodo, M., Nakata, Y., Yoshimoto, N., et al.: Basic research on the mechanical behavior of methane hydrate-sediments mixture. *J. Jpn. Geotech. Soc. Soils Found.* **45**(1), 75–85 (2005)
4. Miyazaki, K., Tenma, N., Aoki, K., et al.: A nonlinear elastic model for triaxial compressive properties of artificial methane-hydrate-bearing sediment samples. *Energies* **5**(12), 4057–4075 (2012)
5. Liu, Z., Dai, S., Ning, F., et al.: Strength estimation for hydrate-bearing sediments from direct shear tests of hydrate-bearing sand and silt. *Geophys. Res. Lett.* **45**(2), 715–723 (2018)
6. Cundall, P.A., Strack, O.D.L.: A discrete numerical model for granular assemblies. *Géotechnique* **30**(30), 331–336 (1979)
7. He, J., Jiang, M.J.: Three-dimensional distinct element novel sample-preparing method and mechanical behavior for pore-filling type of methane hydrate-bearing soil. *J. Tongji Univ. (Nat. Sci.)* **44**(5), 709–717 (2016). (in Chinese)
8. Jiang, M.J., Konrad, J.M., Leroueil, S.: An efficient technique for generating homogeneous specimens for DEM studies. *Comput. Geotech.* **30**(7), 579–597 (2003)
9. He, J., Jiang, M.J., Liu, J.: Effect of different temperatures and pore pressures on geomechanical properties of pore-filling type of methane hydrate soils based on the DEM simulations. In: Li, X., et al. (eds.) *Proceeding of the 7th International Conference on Discrete Element Methods 2017, SPPHY*, vol. 188, pp. 827–835. Springer, Singapore (2017)
10. Satake, M.: Fabric tensor in granular materials. In: Vermeer, P.A., Luger, H.J. (eds.) *Proceedings of IUTAM Symposium on Deformation and Failure of Granular Materials 1982*, pp. 63–68. Balkema, Netherlands (1982)
11. Kuhn, M.R., OVAL and OVALPLOT: Programs for analyzing dense particle assemblies with the discrete element method. [http://faculty.up.edu/kuhn/oval/doc/oval\\_0618.pdf](http://faculty.up.edu/kuhn/oval/doc/oval_0618.pdf). Accessed 28 Feb 2018